NATIONAL AERONAUTICS AND SPACE ADMINISTRATION

Technical Report 32-1474

Sensitivity of Explosives to Laser Energy

Vincent J. Menichelli
L. C. Yang

JET PROPULSION LABORATORY
CALIFORNIA INSTITUTE OF TECHNOLOGY
PASADENA, CALIFORNIA

April 30, 1970

NATIONAL AERONAUTICS AND SPACE ADMINISTRATION

Technical Report 32-1474

Sensitivity of Explosives to Laser Energy

Vincent J. Menichelli
L. C. Yang

JET PROPULSION LABORATORY
CALIFORNIA INSTITUTE OF TECHNOLOGY
PASADENA, CALIFORNIA

April 30, 1970

Prepared Under Contract No. NAS 7-100
National Aeronautics and Space Administration

Preface

The work described in this report was performed by Space Ordnance Systems, Inc., under the cognizance of the Propulsion Division of the Jet Propulsion Laboratory.

This investigation was an outgrowth of an SOS-sponsored program under which the feasibility of a laser-initiated explosive system was studied. SOS developed a compact laser source, a fiber optics laser-transfer system, and laser-initiated explosive components. Although the feasibility of a laser-initiated explosive system had been demonstrated, little was known about the initiation mechanism. Under a JPL contract, a separate study was made to determine the sensitivity to laser energy of explosive and pyrotechnic materials of interest to JPL. Another objective was to obtain a better understanding of the initiation mechanism. At the completion of the contract, SOS submitted a final report* describing the tests performed and the results. The present report evaluates the results of the study made for JPL and assesses the practicability of a laser-initiation system for use aboard a spacecraft.

During the performance of the study contract, the authors were employed by SOS and carried out the work plan.

---

*A *Study of the Sensitivity of Pyrotechnic Materials to Laser Energy,* Contract NAS 7-670, Report R-6630, Space Ordnance Systems, Inc., Saugus, Calif., Feb. 28, 1969.

Contents

Tables

Contents (contd)

Tables (contd)

Figures

Abstract

A study has been made to determine the practicability of initiating some common explosives with laser energy. Pulsed ruby and neodymium lasers, in the free-running mode, were the source of energy. The laser pulse was adjusted for 5 J output and externally attenuated. The explosive materials were pressed prior to testing. Primary high explosives and some metal/metal oxide mixtures were easily initiated. However, secondary high explosives were not initiated at the 5-J level under the conditions reported. Reflectivity of the sample surface is of considerable importance to initiation. The relative sensitivity ordering of the explosives tested conformed quite well to the ordering one would expect from other methods of sensitivity testing, i.e., friction, impact, etc., provided that the sensitivity value is adjusted for reflective losses.

Sensitivity of Explosives to Laser Energy

I. Introduction

The effects of laser energy and light from other strong sources on explosive materials have been studied by various laboratories (Refs. 1–3). This report presents and evaluates the results of a study on the sensitivity of several pyrotechnic and explosive materials to laser energy and hypothesizes the mechanisms believed to be operating. The conclusions drawn from the study are intended to give insight into the practicability of a laser system for the initiation of explosive devices aboard a spacecraft.

The pyrotechnic materials selected for study were those typically used in explosive and propellant devices presently found on aerospace vehicles. The sensitivity testing was done with pulsed ruby and neodymium lasers, in the free-running mode, as the source of energy. Results of the tests are tabulated and a sensitivity ordering of the materials tested is given. The effects of a number of variables on explosive sensitivity are examined.

II. Laser Background

The laser is a recent phenomenon with approximately 10 years of history. Extensive research has brought about tremendous progress in this field, and today various lasers are available for practical applications. Lasers are usually classified by their mode of operation and generally fall into the following categories:

(1) The conventional pulsed mode is mainly obtained by using a solid crystal laser such as ruby or neodymium oxide-doped glass. High-powered flash lamps are used to reach the relatively higher thresholds necessary for lasing. The pulse width ranges from a few (10) microseconds to several milliseconds and is determined mainly by the duration of the flash lamp. Energy output can be obtained in kilojoules.

(2) From the conventional pulsed mode, a Q-switched mode can be generated by passive (chemical), mechanical (rotating mirror), or electro-optical (Pockels cell, Kerr cell) means. The pulse-width range is from picoseconds to hundreds of nanoseconds. Peak power ranges from megawatts to gigawatts and energy from millijoules to about one hundred joules.

(3) A continuous wave (CW) mode is obtained from gas lasers (He–Ne, A, CO_2) and from solid lasers

such as yttrium aluminum garnet (YAG). The average power from these lasers ranges from milliwatts to several hundred watts. (Also available are high-repeat-rate Q-switched lasers.)

In practice, the laser is used to project a high-intensity, coherent beam of radiation. Some of the applications have been to use the intense energy to illuminate, melt, weld, perforate, or ignite materials. For this report, we are concerned primarily with the ability of laser energy to cause ignition of pyrotechnic materials.

The mechanism of initiation of explosives by laser energy can be considered a thermal phenomenon; i.e., light energy is absorbed and converted to heat as witnessed in the application of lasers to welding and drilling. Of the three categories described above, the conventional pulsed-mode laser best meets the requirements of size, energy output, and compatibility with fiber optics for use in a laser/explosive system. In this application, a neodymium laser is the choice over ruby because it is more efficient than the ruby. The other two categories have limitations that obviate their use for this purpose. The energy from a Q-switched ruby or neodymium laser is known to be very difficult to transmit through fiber optics because the high power rate induces serious burning at the laser rod/fiber optics interface. A CW laser is very inefficient and to generate temperatures on a solid surface high enough for this application would be impractical.

Initiation of explosives by light was under study before the invention of the laser (Ref. 3). The light sources used were xenon flash lamps, which inherently contain a number of disadvantages. The light output from a flash lamp is divergent and the light intensity decreases very rapidly as a function of distance. The limits to which the flash lamp can be driven require the sample under test to be placed quite close to the lamp. Furthermore, the output wavelengths are not constant at different energy levels, and explosive sensitivity responses vary accordingly.

By comparison, the advantages of laser-generated energy are primarily that the flux density equated in watts/unit area is much greater; the laser output has a relatively small beam divergence, approximately 5 mrad or less; attenuation of the beam in air is very small; an accurate energy determination is easily made with an energy-absorptive-type calorimeter; and the laser beam is well defined and can be easily focused. It is also quite simple to integrate the energy by absorption because the laser spectral band is very narrow, approximately 100 Å spread. However, lasers have limitations in that there is no unified set of data on certain parameters because they depend upon the construction of the particular laser; e.g.:

(1) Pulse length. We define the pulse length as the time from the first to the last oscillation (spike). The pulse length, amplitude (spike), and frequency increase with energy. The limit of the pulse length is that of the flash lamp and a linear relationship with laser energy is not apparent.

(2) Beam homogeneity. It is known that the output from a solid laser is not homogeneous. For the most symetrically pumped laser (helical lamp and diffuse cavity reflector), the energy distribution is Gaussian with the highest energy density ($J/in.^2$) occurring approximately at the center of the beam. This is commonly referred to as the "hot spot" and its position is approximately the same for different energy levels. It has also been observed that the hot-spot energy density does not vary linearly with total laser energy. That is, at low energy (near threshold) almost the entire energy is contained within the hot spot.

III. Laser Ignition vs Electrical Ignition

The concept of laser ignition of explosive components on board a space vehicle would necessitate a three-part system: a device to generate the laser energy, a means to convey it, and an explosive component to accept and react to the laser energy. The potential advantages of such a system over presently used electrical methods of initiation are increased safety and reliability. Serious safety problems are associated with electroexplosive devices (EED) because of electromagnetic radiation and spurious electrical signals. Inherent to all spacecraft and launch systems are long electrical cables and powerful radio and radar transmitting devices. Electrically initiated explosive devices contain wire bridge circuits and electrical cables capable of picking up spurious signals by induction and/or electromagnetic radiation by coupling. Numerous reports have been recorded of inadvertent initiation of EEDs by "cross talk" in the electrical cables or by pickup of electromagnetic radiation (Ref. 4). These problems have led to the development of 1-W/1-A no-fire and exploding bridgewire devices. These explosive components have reduced susceptibility to inadvertent initiation. However, the complexity of these devices has resulted in costs much higher than conventional EEDS to achieve the same degree of reliability.

Increased safety can be achieved because the laser provides a unique form of energy. In general, materials have not been observed to lase naturally or expected to lase except under very deliberate and positive means. Laser-initiated devices would not contain electrical circuits or be directly tied into electrical equipment. Therefore, they would be immune to the electrical environments associated with space vehicles. All the safeguards now necessary to achieve electrical immunity in the construction of EEDs can be eliminated. This would lead to increased reliability because of the resulting simplicity of the laser-initiated device. The laser-initiated device would consist of a metal body to contain the explosive material and a window through which the laser energy would enter. Piping of the laser energy from the laser source to individual explosive components is possible with the use of nonconductive fiber optics.

IV. Design of the Experiment

The investigation was primarily directed to determine the sensitivity of a number of pyrotechnic materials irradiated by a neodymium laser (wavelength 10,600 Å). One exception was SOS-108 mix (a pyrotechnic mixture) whose sensitivity was also determined with a ruby laser (wavelength 6,943 Å). Materials tested are listed in Table 1. The list includes conductive mixtures, primary high explosives, secondary high explosives, delay mixtures, and propellants. A number of variables listed below and their effect on sensitivity were also examined:

(1) Particle size.

(2) Compaction pressure.

(3) Laser pulse length.

(4) Area of laser beam directed on the sample.

The pyrotechnic materials were loaded into a steel ring as shown in Fig. 1. An inside diameter of 0.4 in. for the sample holder was selected because the diameter of the laser rod is approximately 0.4 in. However, owing to beam divergence, the beam diameter at the test sample (33 in. from the laser rod) would be slightly larger. Five samples, for each condition cited above, were loaded for each explosive material. The sensitivity was to be determined by a fire, no-fire approach. In those cases in which the sample could not be initiated at the upper energy limit of the equipment, an attempt was made to initiate the material by lensing the energy. Before each test the laser was fired into a calorimeter to determine the exact number of joules emitted.

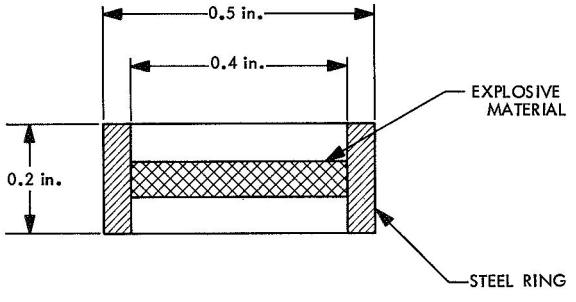

Fig. 1. Sample holder

Table 1. Pyrotechnic materials studied

No.	Material
1	SOS-108 mix[a]
2	Zr-$KClO_4$, 98% with silicone resin, 2% GE silicone resin in GE-SRg8
3	Boron pellets (B/KNO_3)
4	Mg/Teflon pellets
5	ALCLO No. 1 lead
6	ALCLO No. 2 iron
7	Delay mix 176[a]
8	Delay mix 177[a]
9	Lead azide (dextrinated)
10	Polyvinyl alcohol lead azide
11	Lead styphnate
12	PETN
13	RDX
14	DIPAM
15	HMX
16	HNS
17	Saturethane propellant, metallized, as cast
18	Saturethane propellant, nonmetallized, as cast
19	Polyurethane propellant, metallized, as cast
20	Polyurethane propellant AS18, machined
21	Polyurethane propellant AS19, machined
22	Polyurethane propellant AS20, machined

[a]Space Ordnance Systems, Inc., proprietary mixture.

Periodic examination of the explosives loaded into the steel rings showed no serious relaxation of the powder with time. The criteria used were the color and surface finish of the explosive sample. In one case, ALCLO No. 2 iron showed some rusting on the surface.

The tests were conducted at atmospheric pressure. Test conditions did not allow for the containment of reaction products (gases), which would result in high pressures conducive to the propagation of explosive and pyrotechnic reactions. Therefore it is to be expected that the energy levels required for initiation under these conditions will be greater than those required in an obturated system. However, off-setting this limitation somewhat is the window used in a laser-initiated device. If the explosive material is pressed against the window, some of the heat generated on the surface of the explosive will be lost to the window material, with corresponding effect on sensitivity.

The effect on sensitivity as a function of area of the beam was determined by using a stop aperture over the sample. The aperture reduced the area of the beam by 95%, beam divergence not considered. It was observed that the sensitivity of a particular explosive to laser energy did not change significantly with reduction in laser beam area, provided that the near center of the beam was transmitted through the aperture. This technique turned out to be a simple way to verify the existence of hot spots within the laser beam.

It was of interest to determine the effects of laser pulse width on sensitivity. The pulse duration—one approximately 500 μs, one approximately 1.5 ms—was controlled by variations in laser design, such as flash tube, inductance, and capacitance.

Another parameter investigated was the reflectivity of pressed explosives at the ruby and neodymium frequencies. A Bausch and Lomb Spectronic 505 was used. The instrument covered the ruby laser wavelength of 6,943 Å. However, data at the neodymium laser wavelength (10,600 Å) were obtained with a special test fixture in which a CW yttrium aluminum garnet laser, which has a wavelength of 10,600 Å, was used. The fixture, shown in Fig. 2, has the same basic features as the setup for the ruby in that a continuous readout is available from the light source to verify that the source keeps a constant output during the test.

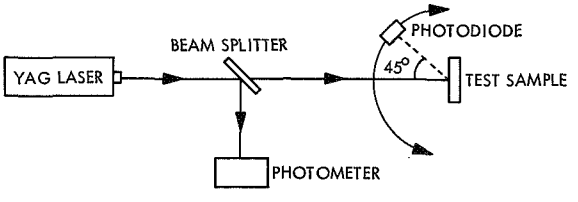

Fig. 2. Reflectance test arrangement

A magnesium oxide block was inserted in the sample holder, and the resulting diode output corresponded to 100% reflection. When a black-light trap was inserted in the sample holder, the output corresponded to 0% reflection. The test samples gave an output somewhere between 100% and 0% reference. The neodymium frequency measurements were made at 45 deg.

Other areas of interest not directly related to the sensitivity study, but of interest from the standpoint of laser application to explosive components, were also considered. A great deal of pressure bomb data on the Apollo Standard Initiator was available and it was of interest to know whether the ignition characteristics would vary as a function of the mechanism of initiation; i.e., electrical initiation or laser initiation. Another area of interest was the sensitivity of some of the materials in Table 1 to laser energy when they are confined in a housing designed for a specific explosive application. Several tests were conducted in these areas and are reported in the next section.

V. Test Results

To better appreciate and understand the sensitivity results it will be advantageous to first review the reflectance data. All materials were tested for reflectivity at 10,600 Å with the exception of SOS-108 mix, which was also tested at 6,943 Å. Table 2 lists the reflectance percentages for SOS-108 mix under the various loading conditions at 6,943 Å. The SOS-108 mix is a powder, dark gray in color, and is expected to be a relatively good light absorber. Table 3 lists the same type of data obtained at a wavelength of 10,600 Å on most of the materials studied. The data show that there is a considerable variation in reflectivity among the samples tested. Some showed very little difference in reflectivity as a function of pressure and particle size. It is recognized that particle size, loading pressure, binder, and surface finish will play a part in the reflectivity of the sample. In the design of laser-initiated devices these parameters will have to be taken into consideration.

Table 2. Reflectance results for SOS-108 mix at 6943 Å

Particle size, mesh	Loading pressure, 10^3 psi	Reflectance, %
Through 100	10	13.5
Through 100	50	13.0
Through 400	10	13.9
Through 400	50	17.2

Table 3. Results of reflectance tests at 10,600 Å

Material	Particle size, mesh	Loading pressure, 10^3 psi	Reflectance, %
SOS-108 mix	Through 100 $KClO_4$	10	10.5
	Through 100 $KClO_4$	50	13.2
	Through 400 $KClO_4$	10	8.8
	Through 400 $KClO_4$	50	11.1
Zr-$KClO_4$	Through 100 $KClO_4$	10	10.5
	Through 100 $KClO_4$	50	11.0
	Through 400 $KClO_4$	10	10.7
	Through 400 $KClO_4$	50	11.5
Boron pellets (B/KNO_3)	Unknown	10	6.2
	Unknown	50	7.2
Mg/Teflon pellets	Unknown	10	82.3
	Unknown	50	83.0
ALCLO No. 1 lead	Unknown	10	90.5
	Unknown	50	92.0
ALCLO No. 2 iron	Unknown	10	24.0
	Unknown	50	44.0
Delay mix 176	Unknown	5	34.0
	Unknown	10	31.8
Delay mix 177	Unknown	5	46.1
	Unknown	10	44.5
Lead azide (dextrinated)	Unknown	2	86.3
	Unknown	10	79.3
Polyvinyl alcohol lead azide	Unknown	2	85.5
	Unknown	10	86.5
Lead styphnate	Through 100	2	65.3
	Through 100	10	76.8
PETN	Class 1	10	88.5
	Class 4	10	71.0
RDX	Through 325	10	80.3
	Through 60–100	50	73.6
DIPAM	Unknown	10	94.0
HMX	Through 325	10	80.0
HNX	Through 325	10	87.8
Saturethane propellant, as cast			
Metallized	Unknown	Cast	11.0
Nonmetallized	Unknown	Cast	33.0
Polyurethane propellant, as cast			
Metallized	Unknown	Cast	12.0
AS18 Machined	Unknown	Cast	†
AS19 Machined	Unknown	Cast	†
AS20 Machined	Unknown	Cast	†

†Reflectivity samples not supplied.

The sample holder was designed to result in an explosive surface area equal to the area of the laser rod diameter. The explosive material was pressed into a thin wafer to minimize the total amount of explosive in the holder. During the reflectivity tests some of the high explosives such as RDX, HMX, and PETN were found to be translucent to laser energy. This is evident since each single crystal is transparent (visible spectrum at least). Irradiation of pressed fine power of these materials resulted in diffusive transmission as witnessed by light-scattering experiments performed with a CW He–Ne laser. In these experiments, a piece of exposed Polaroid film was placed behind pressed, 30-mil-thick samples of the above materials. Energy transmission through the sample was evident from a color change in the film after a focused laser beam was directed on the surface of the sample. It was felt that an error would be introduced in the sensitivity tests if these materials were tested in this manner because some of the laser energy would be transmitted through the sample. To overcome this problem a modified sample holder, shown in Fig. 3, was constructed. The same explosive weight as used in the original sample holder fills the longer-length, smaller-diameter cavity of the modified holder, and thus rules out loss of laser energy by transmission through the sample. The smaller inside diameter is compatible with the sensitivity testing of RDX, HMX, and PETN because in these tests the laser beam was lensed to a smaller diameter.

The technique of determining laser sensitivity was to vary the energy of the laser beam by varying the potential on the capacitor that functioned the flash lamp. However, it was observed that the laser pulse width varied directly with capacitor potential. To obtain a constant pulse width it was then decided to maintain the potential on the capacitor at a fixed voltage. Attenuation of the energy was then achieved externally.

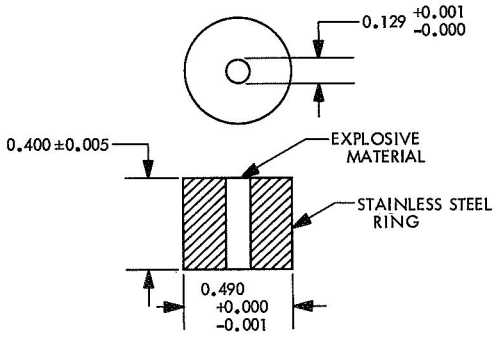

Fig. 3. Modified sample holder

The potential on the capacitor was fixed to result in a laser energy output of 5 J. To attenuate the energy, varying numbers of glass disks (Corning glass 0211, 1.0 in. in diameter and 6 mils thick) were placed in an aluminum holder and set in the axis of the laser beam. A theoretical calculation for transmission, based on the Fresnel reflection formula, is expressed as

$$T = \left[1 - \left(\frac{n-1}{n+1}\right)^2\right]^2,$$

where

T = transmission,

n = the index of refraction of the glass (typical or effective value 1.50).

The disks are placed at a slight angle to the axis of the beam and randomly unparallel to each other. The resulting multireflections are dispersed and do not reach the test sample. The disks were calibrated by three different methods:

(1) Photometric measurements (Bausch & Lomb 505). The results showed no wavelength dependence over the range of the instrument (2,000–8,000 Å) on the transmission factor. It was felt that this could be extrapolated to 10,600 Å.

(2) Continuous laser wave with Ne–He laser (6,293 Å) and YAG laser (10,600 Å). The use of a CW laser in conjunction with a photodiode-type photometer makes a very accurate method of calibration; however, the ruby wavelength 6,943 Å is slightly different from the Ne–He laser wavelength. The results showed no angular dependence up to 30 deg (the maximum angle tested).

(3) Pulsed laser method with ruby and neodymium lasers. Attenuation was measured with a Korad KJ-2 calorimeter. The accuracy was not very good at high attenuation because the calorimeter was limited to ±0.1 J.

Some pertinent details about the pulsed ruby and neodymium lasers are given in the Appendix.

In the process of calibrating the glass disks a piece of exposed Polaroid film was placed 33 in. from the laser rod (the same as the distance from the laser rod to the explosive samples). Each laser pulse for a given attenuation or number of glass disks inserted in the axis of the beam resulted in an etched beam pattern on the film.

From this pattern the area of the beam was measured and the average energy density (J/in.^{2}) calculated.

To equate the true energy density, it was necessary to know the sensitivity of the exposed film (Polaroid type 410). Although this is a general technique used by many investigators, the quantitative sensitivity of the exposed film was not known (Ref. 5). This was determined with the use of linear flash xenon lamps and the Korad calorimeter. The condensing lens of the calorimeter was replaced by a glass plate to compensate for the reflection losses of the lens. The flash lamp output level was set so that the spectral distribution was in the range of the calorimeter. The absorptive cell and the film were placed 3 in. from the flash lamp. Exposed Polaroid film has a constant reflectance at about 4,000 Å to 10,600 Å and a clean threshold beyond which uniform discoloration (progressing from black to white) takes place. The pulse length of the flash ranged from 0.7 to 1.5 ms. Paper sensitivity remained constant up to 30 ms when similar tests were conducted with photo flash bulbs as the light source. (Photo flash bulbs have light durations between 20 and 40 ms.) The threshold energy to cause first indications of discoloration of the film was determined to be 8.5 J/in.^{2}. The exposed film was not sensitive to focused CW light such as photo flood lamps or sunlight.

With knowledge of the film sensitivity, it is possible to determine an attenuation factor, i.e., the attenuation required to just cause the laser energy (hot spot) to disappear from the film. From this the density (J/in.^{2}) of the hot spot in the beam for any attenuation can be determined. The following expression is used to calculate the hot-spot density:

$$D = \frac{8.5 \times T}{T_F},$$

where

D = hot-spot density, J/in.^{2},

T = transmission,

T_F = last transmission level at which film was affected.

The ruby laser adjusted to 5.0 J output gave a pulse width of 1.6 ms. With the glass disks used for attenuation purposes, the calibration data in Table 4 were generated. The neodymium pulse width was 1.5 ms in duration at 5.0 J output. The results of this calibration are given in Table 5.

Numerous attempts were made, without success, to obtain a short-duration pulse (approximately 500 μs) with the ruby rod. To achieve this it would be necessary that the RC time constant be significantly reduced. Since the value of R is fixed by the flash lamp the only variable is the capacitance. If the capacitance is reduced, the potential must be increased to maintain constant energy. The result was to increase the potential above the self-flash point and operating limit of the xenon lamp. This limiting factor left a pulse still in excess of 500 μs. It was therefore decided to obtain the shortest possible ruby pulse with the Korad equipment. It was found that a laser pulse duration of 1.1 ms could be obtained when the lower input potential was fixed at 3450 V, which resulted in a laser energy output of 0.43 J. With these conditions the laser was calibrated as described earlier, with results as summarized in Table 6.

To obtain the short-duration (500 μs) laser pulse with the neodymium rod a different approach was used. The Korad equipment was modified by replacing the helical xenon lamp with a linear xenon lamp and omitting the water-cooling feature. Details of this system are given in the Appendix. At the 5-J output level, the pulse duration is 450 μs. Calibration data for the system are summarized in Table 7.

From the data compiled in Tables 4 through 7, a profile of the energy density in the beam, at 33 in., was plotted as a function of the radial position. Figures 4 through 7 show beam patterns* assumed to be symmetrical and circular in shape. The irregular Gaussian distribution is believed to be due to excitation of transverse as well as axial modes (Ref. 6). The unattenuated beam diameter is larger than the diameter of the rod, as expected, because of beam divergence (3 to 5 mrad typical value). An integration of the energy from the profiles accounts for approximately 60% of the laser energy. The remainder would have to be accounted for in the area below the film sensitivity.

Testing of the explosive materials generated a great deal of data. Tables 8 through 19 report the data under the various conditions tested. Items 12 through 22 of Table 1 were tested in the same manner as the other

*The plots in Figs. 4 through 7 were created by a technique called Projectograph. Technology Service Corporation of Santa Monica, California, provides a complete set of FORTRAN computer programs for plotting three-dimensional projections of single-valued surfaces. Then hidden-line logic is used to plot only that portion of each "cut" that is visible.

Table 4. Calibration of glass disks with the ruby laser and resultant hot-spot density; pulse width, 1.6 ms

No. of glass disks	*T* (theoretical),[a] %	*T* (experimental),[a] %	Laser energy, J	Average beam diameter, in.	Area of beam, in.^{2}	*D*,[b] J/in.^{2}
0	100	100	5.0	0.468	0.172	53.1
1	92.0	91.8	4.6	0.454	0.162	48.8
2	84.64	84.0	4.3	0.445	0.152	44.6
3	77.87	77.0	3.8	0.438	0.150	40.9
4	71.64	71.5	3.55	0.404	0.128	38.0
5	65.91	65.0	3.25	0.382	0.115	34.5
6	60.64	61.0	3.05	0.372	0.108	32.4
7	55.79	55.5	2.75	0.339	0.093	29.5
8	51.33	52.0	2.6	0.334	0.087	27.6
9	47.22	47.0	2.35	0.323	0.082	25.0
10	43.44	43.5	2.15	0.309	0.075	23.1
11	39.96	40.0	2.0	0.305	0.073	21.3
12	36.76	36.0	1.8	0.288	0.065	19.1
13	33.82	33.0	1.64	0.281	0.062	17.5
14	31.11	30.0	1.5	0.265	0.055	15.9
15	28.62	28.0	1.4	0.239	0.045	14.9
16	26.33	26.0	1.3	0.178	0.025	13.8
17	24.22	24.0	1.2	0.164	0.021	12.8
18	22.28	22.0	1.1	0.129	0.013	11.7
19	20.49	20.0	1.0	0.118	0.011	10.6
20	18.85	19.0	0.95	0.105	0.0087	10.1
21	17.34	17.5	0.87	0.080	0.005	9.3
22	15.95	16.0	0.8	0.056	0.0025	8.5
23	14.67	14.0	0.7		—	

[a] *T* = transmission.

[b] *D* = hot-spot energy density.

Table 5. Calibration of glass disks with the neodymium laser and resultant hot-spot density; pulse width, 1.5 ms

No. of glass disks	*T* (theoretical),[a] %	*T* (experimental),[a] %	Laser energy, J	Average beam diameter, in.	Area of beam, in.^{2}	*D*,[b] J/in.^{2}
0	100	100	5.0	0.438	0.150	44.7
1	92.0	92.5	4.65	0.429	0.145	41.4
2	84.64	84.5	4.35	0.423	0.140	37.8
3	77.87	78.0	3.90	0.411	0.132	34.9
4	71.64	71.5	3.56	0.394	0.122	32.0
5	65.91	66.0	3.30	0.382	0.115	29.5
6	60.64	60.5	3.04	0.372	0.108	27.1
7	55.79	56.0	2.80	0.353	0.098	25.1
8	51.33	51.5	2.57	0.330	0.085	23.0
9	47.22	47.5	2.37	0.309	0.075	21.3
10	43.44	43.5	2.17	0.283	0.063	19.5
11	39.96	40.0	2.0	0.245	0.047	17.9
12	36.76	36.5	1.83	0.225	0.040	16.3
13	33.82	34.0	1.7	0.217	0.037	15.2
14	31.11	31.5	1.58	0.210	0.035	14.1
15	28.62	28.5	1.42	0.171	0.023	12.8
16	26.33	26.5	1.32	0.160	0.020	11.9
17	24.22	24.5	1.23	0.118	0.011	11.0
18	22.28	22.5	1.12	0.097	0.0075	10.1
19	20.49	20.5	1.02	0.080	0.005	9.2
20	18.85	19.0	0.95	0.056	0.0025	8.5
21	17.34	17.5	0.87			7.8

[a] *T* = transmission.
[b] *D* = hot-spot energy density.

Table 6. Calibration of glass disks with the ruby laser and resultant hot-spot density; pulse width, 1.1 ms

No. of glass disks	*T* (theoretical),[a] %	*T* (experimental),[a] %	Laser energy, J	Average beam diameter, in.	Area of beam, in.^{2}	*D*,[b] J/in.^{2}
0	100	100	0.43	0.167	0.0225	18.1
1	92.0	91.9	0.39	0.153	0.0188	16.6
2	84.64	84.0	0.36	0.132	0.0138	15.2
3	77.87	77.5	0.33	0.126	0.0125	14.0
4	71.64	71.5	0.31	0.118	0.0112	12.9
5	65.91	65.5	0.28	0.106	0.0088	11.8
6	60.64	61.0	0.26	0.098	0.0076	11.0
7	55.79	55.5	0.24	0.089	0.0062	10.0
8	51.33	51.5	0.22	0.056	0.0025	9.3
9	47.22	47.0	0.20	0.046	0.0017	8.5
10	43.44	43.5	0.18		—	

[a] *T* = transmission.
[b] *D* = hot-spot energy density.

Table 7. Calibration of glass disks with the neodymium laser and resultant hot-spot density; pulse width, 450 μs

No. of glass disks	T (theoretical),[a] %	T (experimental),[a] %	Laser energy, J	Average beam diameter, in.	Area of beam, in.^{2}	D,[b] J/in.^{2}
0	100	100	5.0	0.476	0.178	80.2
1	92.0	92.3	4.62	0.458	0.165	74.0
2	84.64	84.5	4.22	0.445	0.152	67.8
3	77.87	78.0	3.90	0.430	0.146	62.5
4	71.64	71.6	3.58	0.420	0.138	57.4
5	65.91	66.0	3.30	0.407	0.130	52.9
6	60.91	60.5	3.06	0.399	0.125	48.5
7	55.79	56.0	2.80	0.382	0.115	44.9
8	51.33	51.5	2.57	0.378	0.112	41.3
9	47.22	47.5	2.37	0.363	0.102	38.1
10	43.44	43.5	2.16	0.356	0.100	34.9
11	39.96	40.0	2.0	0.353	0.097	32.1
12	36.76	36.6	1.82	0.339	0.093	29.3
13	33.82	34.0	1.70	0.338	0.090	27.3
14	31.11	31.5	1.58	0.334	0.087	25.3
15	28.62	28.7	1.43	0.323	0.082	23.0
16	26.33	26.5	1.33	0.313	0.077	21.2
17	24.22	24.1	1.21	0.303	0.072	19.3
18	22.28	22.1	1.10	0.276	0.060	17.7
19	20.49	20.5	1.02	0.234	0.043	16.4
20	18.85	18.7	0.97	0.220	0.038	15.0
21	17.34	17.5	0.88	0.205	0.033	14.0
22	15.95	16.0	0.80	0.196	0.030	12.8
23	14.67	14.8	0.74	0.178	0.025	11.9
24	13.49	13.5	0.67	0.149	0.018	10.8
25	12.41	12.5	0.63	0.129	0.013	10.0
26	11.41	11.5	0.58	0.113	0.010	9.2
27	10.55	10.6	0.53	0.097	0.0075	8.5
28	9.66	9.5	0.47		—	7.6

[a] T = transmission.

[b] D = hot-spot energy density.

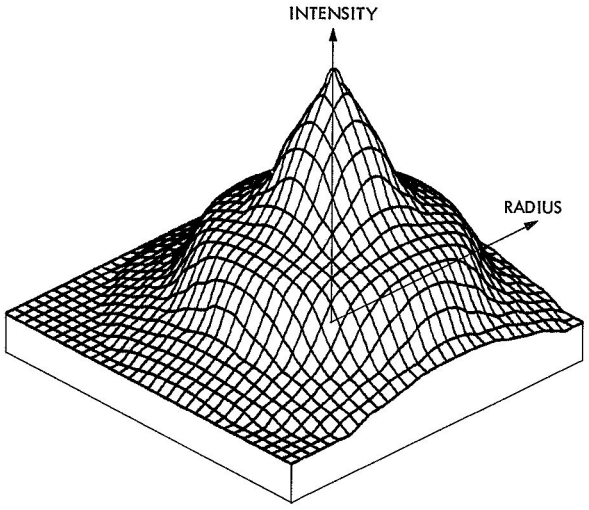

Fig. 4. Laser-energy profile for ruby laser; pulse width, 1.6 ms

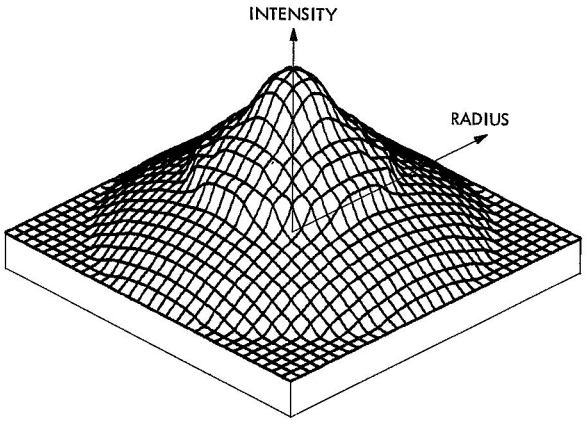

Fig. 5. Laser-energy profile for neodymium laser; pulse width, 1.5 ms

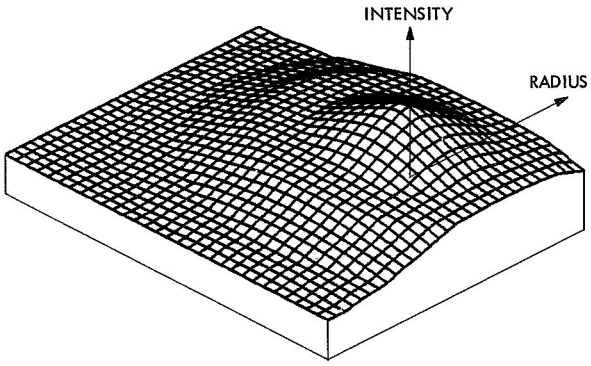

Fig. 6. Laser-energy profile for ruby laser; pulse width, 1.1 ms

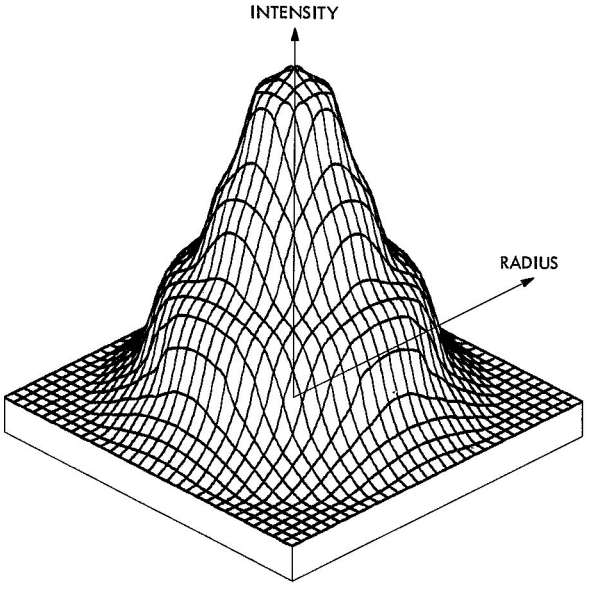

Fig. 7. Laser-energy profile for neodymium laser; pulse width, 450 μs

Table 8. Mean energy and energy density to initiate SOS-108 mix with the ruby laser

Particle size, mesh	Reflectance, %	Unit	Full beam		Partial beam	
			Short pulse (1.1 ms)	Long pulse (1.6 ms)	Short pulse (1.1 ms)	Long pulse (1.6 ms)
Through 100	13.9	Loading pressure: 10,000 psi				
		Energy, J	0.25	1.0	0.27	1.22
		Energy density, $J/in.^2$	10.5	10.6	11.4	13.0
Through 400	13.5	Energy, J	0.31	1.22	0.3	1.28
		Energy density, $J/in.^2$	13.0	13.0	12.6	13.6
Through 100	17.2	Loading pressure: 50,000 psi				
		Energy, J	0.33	1.16	0.32	1.43
		Energy density, $J/in.^2$	13.9	12.3	13.5	15.2
Through 400	13.0	Energy, J	0.4	1.59	0.4	1.62
		Energy density, $J/in.^2$	16.8	16.9	16.8	17.2

Table 9. Mean energy and energy density to initiate SOS-108 mix with the neodymium laser

Particle size, mesh	Reflectance, %	Unit	Full beam		Partial beam	
			Short pulse (450 μs)	Long pulse (1.5 ms)	Short pulse (450 μs)	Long pulse (1.5 ms)
Through 100	10.5	Loading pressure: 10,000 psi				
		Energy, J	0.58	1.11	0.58	1.27
		Energy density, $J/in.^2$	9.3	9.9	9.3	11.4
Through 400	8.8	Energy, J	0.74	1.46	0.74	1.43
		Energy density, $J/in.^2$	11.9	13.1	11.9	12.8
Through 100	13.2	Loading pressure: 50,000 psi				
		Energy, J	0.79	1.43	0.76	1.40
		Energy density, $J/in.^2$	12.9	12.8	12.2	12.5
Through 400	11.1	Energy, J	0.93	1.80	0.95	2.07
		Energy density, $J/in.^2$	14.9	16.1	15.2	18.5

Table 10. Mean energy and energy density to initiate Zr-$KClO_4$ mix with the neodymium laser

Particle size, mesh	Reflectance, %	Unit	Full beam		Partial beam	
			Short pulse (450 μs)	Long pulse (1.5 ms)	Short pulse (450 μs)	Long pulse (1.5 ms)
Through 100	10.5	Loading pressure: 10,000 psi				
		Energy, J	0.48	0.98	0.49	0.95
		Energy density, J/in.^{2}	7.7	8.8	7.9	8.5
Through 400	10.7	Energy, J	0.48	0.87	0.48	0.85
		Energy density, J/in.^{2}	7.7	7.8	7.7	7.6
Through 100	11.0	Loading pressure: 50,000 psi				
		Energy, J	0.54	0.96	0.48	0.95
		Energy density, J/in.^{2}	8.6	8.6	7.7	8.5
Through 400	11.5	Energy, J	0.53	0.95	0.53	0.96
		Energy density, J/in.^{2}	8.5	8.5	8.5	8.5

Table 11. Mean energy and energy density to initiate boron pellets (B/KNO_3) with the neodymium laser

Particle size, mesh	Reflectance, %	Unit	Full beam		Partial beam	
			Short pulse (450 μs)	Long pulse (1.5 ms)	Short pulse (450 μs)	Long pulse (1.5 ms)
Unknown	6.2	Loading pressure: 10,000 psi				
		Energy, J	1.10	1.01	1.22	1.02
		Energy density, J/in.^{2}	17.6	9.0	19.6	9.1
Unknown	7.2	Loading pressure: 50,000 psi				
		Energy, J	2.15	1.72	2.39	1.71
		Energy density, J/in.^{2}	34.5	15.4	38.3	15.3

Table 12. Mean energy and energy density to initiate Mg/Teflon pellets with the neodymium laser

Particle size, mesh	Reflectance, %	Unit	Full beam		Partial beam	
			Short pulse (450 μs)	Long pulse (1.5 ms)	Short pulse (450 μs)	Long pulse (1.5 ms)
Unknown	82.3	Loading pressure: 10,000 psi				
		Energy, J	5.5	3.35	5.4	3.24
		Energy density, J/in.^{2}	88.2	29.9	86.6	30.0
Unknown	83.0	Loading pressure: 50,000 psi				
		Energy, J	5.5[a]	13.0	5.5[a]	13.0
		Energy density, J/in.^{2}	>100	74.5	>100	74.5

[a]Beam was lensed.

Table 13. Mean energy and energy density to initiate ALCLO No. 1 lead with the neodymium laser

Particle size, mesh	Reflectance, %	Unit	Full beam		Partial beam	
			Short pulse (450 μs)	Long pulse (1.5 ms)	Short pulse (450 μs)	Long pulse (1.5 ms)
Unknown	90.5	Loading pressure: 10,000 psi				
		Energy, J	1.80	2.6	1.7	2.57
		Energy density, J/in.^{2}	28.9	23.2	27.3	23.0
Unknown	92.0	Loading pressure: 50,000 psi				
		Energy, J	3.50	7.4	3.82	7.4
		Energy density, J/in.^{2}	56.1	66.2	61.3	66.2

Table 14. Mean energy and energy density to initiate ALCLO No. 2 iron with the neodymium laser

Particle size, mesh	Reflectance, %	Unit	Full beam		Partial beam	
			Short pulse (450 μs)	Long pulse (1.5 ms)	Short pulse (450 μs)	Long pulse (1.5 ms)
Unknown	24.0	Loading pressure: 10,000 psi				
		Energy, J	2.57	3.2	2.55	3.25
		Energy density, J/in.^{2}	41.2	28.6	40.9	29.1
Unknown	44.0	Loading pressure: 50,000 psi				
		Energy, J	4.2	7.15	4.65	7.10
		Energy density, J/in.^{2}	67.4	63.9	74.6	63.5

Table 15. Mean energy and energy density to initiate delay mix 176 with the neodymium laser

Particle size, mesh	Reflectance, %	Unit	Full beam		Partial beam	
			Short pulse (450 μs)	Long pulse (1.5 ms)	Short pulse (450 μs)	Long pulse (1.5 ms)
Unknown	34.0	Loading pressure: 5,000 psi				
		Energy, J	0.87	1.59	0.87	1.59
		Energy density, J/in.^{2}	14.0	14.2	14.0	14.2
Unknown	31.8	Loading pressure: 10,000 psi				
		Energy, J	0.95	1.56	0.86	1.54
		Energy density, J/in.^{2}	15.2	13.9	13.8	13.8

Table 16. Mean energy and energy density to initiate delay mix 177 with the neodymium laser

Particle size, mesh	Reflectance, %	Unit	Full beam		Partial beam	
			Short pulse (450 μs)	Long pulse (1.5 ms)	Short pulse (450 μs)	Long pulse (1.5 ms)
Unknown	46.1	Loading pressure: 5,000 psi				
		Energy, J	1.22	2.17	1.32	2.17
		Energy density, J/in.^{2}	19.6	19.4	21.2	19.4
Unknown	44.5	Loading pressure: 10,000 psi				
		Energy, J	1.43	2.35	1.43	2.38
		Energy density, J/in.^{2}	22.9	21.0	22.9	21.3

Table 17. Mean energy and energy density to initiate lead azide (dextrinated) with the neodymium laser

Particle size, mesh	Reflectance, %	Unit	Full beam		Partial beam	
			Short pulse (450 μs)	Long pulse (1.5 ms)	Short pulse (450 μs)	Long pulse (1.5 ms)
Unknown	36.3	Loading pressure: 2,000 psi				
		Energy, J	1.96	3.6	2.0	3.52
		Energy density, J/in.^{2}	31.4	32.2	32.1	31.5
Unknown	79.3	Loading pressure: 10,000 psi				
		Energy, J	1.60	2.75	1.6	2.75
		Energy density, J/in.^{2}	25.7	24.6	25.7	24.6

Table 18. Mean energy and energy density to initiate polyvinyl alcohol lead azide with the neodymium laser

Particle size, mesh	Reflectance, %	Unit	Full beam		Partial beam	
			Short pulse (450 μs)	Long pulse (1.5 ms)	Short pulse (450 μs)	Long pulse (1.5 ms)
Unknown	85.5	Loading pressure: 2,000 psi				
		Energy, J	1.43	2.65	1.5	2.80
		Energy density, J/in.^{2}	22.9	23.7	24.1	25.0
Unknown	86.5	Loading pressure: 10,000 psi				
		Energy, J	1.30	2.15	1.22	2.12
		Energy density, J/in.^{2}	20.9	19.2	19.4	19.6

Table 19. Mean energy and energy density to initiate lead styphnate with the neodymium laser

Particle size, mesh	Reflectance, %	Unit	Full beam		Partial beam	
			Short pulse (450 μs)	Long pulse (1.5 ms)	Short pulse (450 μs)	Long pulse (1.5 ms)
Through 100	65.3	Loading pressure: 2,000 psi				
		Energy, J	0.56	0.98	0.58	0.98
		Energy density, J/in.^{2}	9.0	8.8	9.3	8.8
Through 100	76.8	Loading pressure: 10,000 psi				
		Energy, J	0.45	0.85	0.53	0.87
		Energy density, J/in.^{2}	7.2	7.6	8.5	7.8

materials, but the samples all failed to initiate at the 5-J level. These samples were further tested with the laser energy increased to 15 J without successful ignition. At the 15-J energy level the beam was focused through a lens, which resulted in an energy density of approximately 1500 J/in.^{2} Under confined conditions, PETN and RDX are known to initiate at density levels of about 50 J/in.^{2} The failure of these materials to ignite at the 1500-J/in.^{2} level is believed to be due to a lack of proper confinement of the explosive. Under the conditions of no confinement, such as in this case, some chemical reaction occurs with considerable breakup of the explosive column. It is postulated that chemical reaction started, but failed to propagate because the reaction products were not confined. Other indications of chemical reaction were color changes and reaction products deposited on the focusing lens located about 1 in. from the explosive sample. If the materials were highly confined in a laser-initiated-type device, the pressure from the reaction products, which supports propagation, would be maintained and a self-propagating reaction might occur.

The materials more sensitive to laser energy, such as SOS-108 mix, lead styphnate, and lead azide, were not affected by particle size, loading pressure, and pulse width. However, for materials which were less sensitive to laser energy, the results indicate that loading pressure appears to affect their sensitivity, which decreases with increased pressure. The materials have been ordered in Table 20 with the material most sensitive to laser initiation first, as measured by the average energy density of all conditions tested. The ordering is quite different than would be expected by comparison with sensitivity to impact, friction, electrostatic discharge, and heat. If one considers the material from the standpoint of laser sensitivity only, then the ordering in Table 20 is valid. However, if we take into consideration the reflectivity of the material, then an ordering more consistent with other methods of sensitivity testing results. Table 21 lists the revised ordering.

A comparison was made of the output (pressure–time P/t characteristics) of a typical electroexplosive device (EED) initiated by laser energy. The Apollo Standard Initiator (ASI) was the EED selected for the test. A second ASI was converted to accept laser energy in lieu of the electrical header. Details of the construction of each device are given in Table 22. The test was conducted by initiating each device in a 10-cm^3 bomb and observing the P/t characteristics with a Kistler 601A transducer. The resultant oscilloscope traces (redrawn) are shown in Fig. 8. The resultant outputs of each appear to be similar.

Table 20. Order of sensitivity of materials to laser energy

Order	Material	Average energy density to initiate,[a] J/in.^{2}
1	Zr-$KClO_4$	8.2
2	Lead styphnate	8.4
3	SOS-108 (neodymium)	12.8
4	SOS-108 (ruby)	13.8
5	Delay mix 176	14.1
6	Boron pellets (B/KNO_3)	19.9
7	Delay mix 177	21.0
8	Polyvinyl alcohol lead azide	21.9
9	Lead azide (dextrinated)	28.5
10	ALCLO No. 1 lead	44.0
11	ALCLO No. 2 iron	51.2
12	Mg/Teflon	73.0

[a]Energy density value is the mean value of all the conditions tested.

Table 21. Sensitivity ordering of materials based on reflectivity

Order	Material	Adjusted energy density to initiate,[a] J/in.^{2}
1	Lead styphnate	2.4
2	Polyvinyl alcohol lead azide	3.1
3	ALCLO No. 1 lead	3.9
4	Lead azide (dextrinated)	4.9
5	Zr-$KClO_4$	7.1
6	Delay mix 176	9.5
7	SOS-108 (neodymium)	11.4
8	SOS-108 (ruby)	12.3
9	Mg/Teflon	12.7
10	Delay mix 177	12.8
11	Boron pellets (B/KNO_3)	18.6
12	ALCLO No. 2 iron	33.8

[a]Adjusted energy density = energy density − (reflectance × energy density).

Table 22. Construction details of initiator devices

Item	ASI	Laser initiator
Energy input	Electric current	Laser energy
Mechanism	Alumina pinheader, 2-mil stainless steel; 304 bridgewire (resistance 1 Ω)	Window (silica)
Primary mix	65 mg SOS-108 pressed at 10^4 psi	65 mg SOS-108 pressed at 10^4 psi
Secondary mix	60 mg SOS-108, hand pressed	60 mg SOS-108, hand pressed

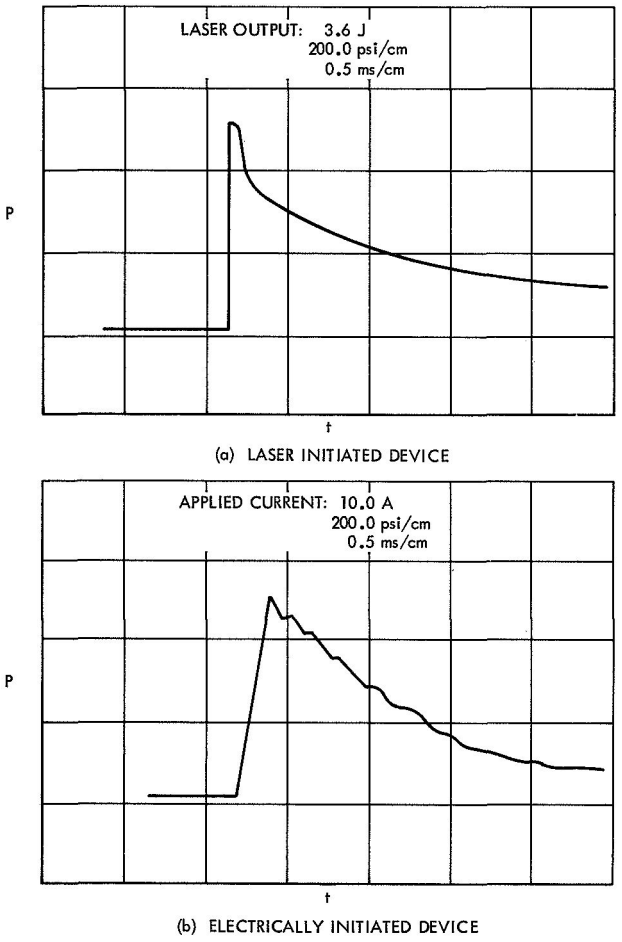

(a) LASER INITIATED DEVICE

(b) ELECTRICALLY INITIATED DEVICE

Fig. 8. Pressure/time traces

It was of interest to test some of the explosive materials in a confined body. The materials were loaded in a device designed to accept laser energy and irradiated with a single laser pulse. Some of the explosive materials were doped, in an attempt to make them more sensitive

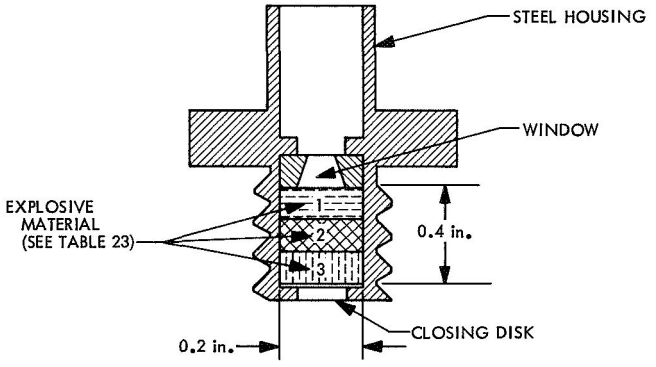

Fig. 9. Laser-initiated explosive device

to laser energy. Figure 9 illustrates the construction of the laser-initiated device. The materials tested and the manner in which they were doped and loaded are given in Table 23. The devices were placed in a safety chamber with a steel witness block next to the output end. By means of an orifice in the safety chamber the laser beam was focused on the window of the device. The distance from the laser rod to the window was 5 in. The energy output of the laser was set at 5 J. Of the samples tested, five initiated: ALCLO No. 2 iron, SOS-108, Mg/Teflon, SOS-108 with 10% microballoons, and Mg/Teflon with 10% microballoons. The samples that were initiated did not cause a dent in the steel blocks, which is reasonable since these materials do not normally detonate. It was expected that SOS-108 mix would ignite because of the past history of this material. It was surprising that B/KNO_3 did not ignite, because Mg/Teflon and ALCLO No. 2 iron, which are less sensitive to laser energy, ignited under the same conditions. There is no explanation of why B/KNO_3 did not ignite.

VI. Discussion

A number of explosive materials have been irradiated with laser energy and a relative ordering of sensitivity constructed. The sample size was small and the sensitivity values are considered approximations. It is believed that with a different laser and test setup, other values would be obtained. However, the sensitivity ordering would be consistent with that obtained in this study.

The laser sensitivity of the material decreases as reflective losses increase. This implies that particle size and shape, color, and surface finish of the explosive material are important parameters to consider. Although

Table 23. Loading details for laser-initiated devices

Explosive material	Dope[a]	Loading pressure, 10^3 psi		
		Increment 1	Increment 2	Increment 3
HNS	—	50	10	10
DIPAM	—	50	10	10
RDX	—	50	10	10
PETN	—	50	10	10
HNS	10% microballoons, 10% methylene blue	10	10	10
DIPAM	10% microballoons	10	10	10
RDX	10% methylene blue	10	10	10
PETN	10% microballoons	10	10	10
AIC10 No. 2 iron	—	10	10	10
SOS-108	—	10	10	10
B/KNO_3	—	10	10	10
Mg/Teflon	—	10	10	10
ALCLO No. 2 iron	10% microballoons	10	10	10
SOS-108	10% microballoons	10	10	10
B/KNO_3	10% microballoons	10	10	10
Mg/Teflon	10% microballoons	10	10	10

[a]Doping in first increment (next to window) only.

some trends in sensitivity appeared with change in explosive-loading density and particle size, the data were not conclusive enough to be convincing. The effect of pulse length on sensitivity was obscure, and further study in this area (including Q-switch pulsing) is needed. It appears that ignition is a function of total energy. Barbarisi and Kessler at Picatinny Arsenal (Refs. 1, 2) show that laser initiation is dependent upon both power and energy.

A very significant observation resulting from this study was the energy distribution within the laser beam. It is known that the laser beam is not homogeneous and appears to have a Gaussian distribution. It would be ideal to have an equal distribution of the energy within the beam. The parameters affecting laser-energy distribution open up a new area of needed investigation. This becomes very apparent as one begins to consider a systems concept of laser-initiated devices requiring fiber optics as an energy-transport vehicle.

It was very interesting to note that the explosive sensitivity did not change as a function of laser-beam area radiated on the sample, provided the hot spot of the beam always illuminated the sample. This raises the question of the mechanism of initiation. On the basis of observations in this study, it is believed (or theorized) that the mechanism is thermal. If we consider the ignition theory of Bowden and Yoffe (Ref. 3) as the mechanism responsible for initiation in this case, the size and intensity of the high-energy density in the laser beam are compatible with the theory. If, in fact, the high-energy density in the laser beam is responsible for initiation, the use of fiber optics raises serious questions. When a fiber optics bundle is divided into multiple outlets for simultaneous initiation of explosive devices from a single laser pulse, an unequal distribution of energy will take place. Unless the energy in the laser pulse far exceeds that needed for initiation, the reliability of the system would be in question.

In keeping with the above remarks on laser-energy distribution within the beam, some explanation of Table 7 and Fig. 7 is warranted. To achieve the short-duration pulse (450 μs) with the neodymium laser it was necessary to use a linear flash lamp. The resultant beam patterns were more irregular than helical lamp patterns and the average beam diameter more difficult to measure. The neodymium laser data in Table 5 and Fig. 5 were obtained with a helical flash lamp. Comparison of the two sets of data—linear flash lamp vs helical flash lamp—shows a different energy distribution when all other parameters are held constant. It is apparent from these data that explosive sensitivity values are dependent upon the specific laser system used.

The feasibility of a laser-initiated explosive system has been successfully demonstrated in the laboratory. However, to adapt it to space or airborne uses demands further investigation. If a laser system is to be considered, the following areas need more study. Environmental problems such as vibration and shock must be considered. Adverse effects on optical alignment, fragile flash lamps, etc., must be overcome. Other areas of concern are laser-beam homogeneity, optimization of fiber optics bundles, interfaces between laser/lens/fiber optics/explosive device, and the design of the laser-initiated explosive device.

VII. Conclusions

Laser initiation of the more sensitive explosive materials is quite feasible. Extension to explosive devices and systems is possible and practicable.

The mechanism of initiation appears to be thermal, although other phenomena may also be at work. The condition of the explosive surface, such as particle size, density, and reflectivity, affects the laser sensitivity of the material.

The high-energy densities within the laser beam were the probable cause of initiation, a conjecture that gives weight to the thermal mechanism of initiation.

References

1. Barbarisi, Modesto J., and Kessler, Edward G., *Initiation of Secondary Explosives by means of Laser Radiation,* Technical Report 3861. Picatinny Arsenal, N.J., May 1969.
2. Barbarisi, Modesto J., and Kessler, Edward G., "Some Initial Investigations of the Laser Initiation of Explosives," in *Preceedings of the Sixth Symposium on Electroexplosive Devices, San Francisco, California,* July 8–10, 1969. The Franklin Institute Research Laboratories, Philadelphia, Pa.
3. Bowden, F. P., and Yoffe, A. D., *Fast Reactions in Solids.* Butterworth's Scientific Publications, London, 1958.
4. Constant, Paul C., Jr., Rhodes, Billy L., and Chambers, George E., *Investigation of Premature Explosions of Electroexplosive Devices and Systems by Electromagnetic Radiation Energy (U).* Midwest Research Institute, Kansas City, Mo., Apr. 1962 (Confidential).
5. *Laser Parameter Measurements Handbook,* Section 4.10.1, p. 122. John Wiley & Sons, Inc., New York, 1968.
6. Kalinin, Yu A., Mak, A. A., and Stepanov, A. I., "Effect of Inverted-Population Distribution on Transverse Laser Modes," *Soviet Physics—Technical Physics,* Vol. 13. No. 7, Jan. 1969.

Appendix

System Specifications of Pulsed Ruby and Neodymium Lasers

I. Ruby Laser

Manufacturer of rod	Linde Division, Union Carbide
Diameter of rod	0.370 in.
Area of end faces	0.108 in.^{2}
Effective length of rod	3.50 in.
Capacitance	400 μF
Flash lamp	Helical xenon
Reflector cavity	White ceramic
Back mirror	100% reflectance at 6943 Å (gold)
Front mirror	50% reflectance at 6943 Å (gold)

II. Neodymium (ED 3) Laser

Manufacturer of rod	Owens-Illinois, Inc.
Diameter of rod	0.40 in.
Area of end faces	0.126 in.^{2}
Effective length of rod	4.0 in.
Capacitance	400 μF
Flash lamp	Helical xenon
Reflector cavity	White ceramic
Back mirror	100% (dielectric coated) at 1.06 μ
Front mirror	65% (dielectric coated) at 1.06 μ

III. Neodymium (ED 3) Short-Pulse Laser

Manufacturer of rod	Owens-Illinois, Inc.
Diameter of rod	0.40 in.
Area of end faces	0.126 in.^{2}
Effective length of rod	4.0 in.
Capacitance	200 μF
Inductance	100 μH
Lamp	EG&G FX 45-4c linear xenon flash lamp OD, 9 mm; ID, 7 mm Arc length, 4.0 in.
Reflector cavity	Close-wrapped aluminum foil (5 mils thick)
Back mirror	100% (dielectric coated) at 1.06 μ
Front mirror	75% (dielectric coated) at 1.06 μ
Cooling	Air cooling with fan near laser head

NASA — JPL — Coml., L.A., Calif.